A&A 672, L2 (2023)
https://doi.org/10.1051/0004-6361/202244822

Astronomy & Astrophysics

LETTER TO THE EDITOR

Venus cloud discontinuity in 2022

The first long-term study with uninterrupted observations

J. Peralta[1], A. Cidadão[2], L. Morrone[3,4], C. Foster[5], M. Bullock[6], E. F. Young[7], I. Garate-Lopez[8], A. Sánchez-Lavega[8], T. Horinouchi[9], T. Imamura[10], E. Kardasis[11], A. Yamazaki[12], and S. Watanabe[13]

[1] Facultad de Física, Universidad de Sevilla, Av. Reina Mercedes s/n, 41012 Sevilla, Spain
e-mail: jperalta1@us.es
[2] Associação Portuguesa de Astrónomos Amadores (APAA), Portugal
[3] AstroCampania, Italy
[4] British Astronomical Association, UK
[5] Astronomical Society of Southern Africa (ASSA), South Africa
[6] Science and Technology Corp., Boulder, CO, USA
[7] Southwest Research Institute, Boulder, CO, USA
[8] Escuela de Ingeniería de Bilbao, Universidad del País Vasco (UPV/EHU), Bilbao, Spain
[9] Faculty of Environmental Earth Science, Hokkaido University, Sapporo, Japan
[10] Graduate School of Frontier Sciences, The University of Tokyo, Tokyo, Japan
[11] Hellenic Amateur Astronomy Association, Athens, Greece
[12] Institute of Space and Astronautical Science, Japan Aerospace Exploration Agency (JAXA), Sagamihara, Japan
[13] Hokkaido Information University, Ebetsu, Japan

Received 27 August 2022 / Accepted 7 February 2023

ABSTRACT

Context. First identified in 2016 by the Japan Aerospace eXploration Agency (JAXA) Akatsuki mission, the discontinuity or disruption is a recurrent wave observed to propagate over decades at the deeper clouds of Venus (47–56 km above the surface), while its absence at the top of the clouds (~70 km) suggests that it dissipates at the upper clouds and contributes to the maintenance of the puzzling atmospheric superrotation of Venus through wave-mean flow interaction.
Aims. Taking advantage of the campaign of ground-based observations undertaken in coordination with the Akatsuki mission from December 2021 until July 2022, we undertook the longest uninterrupted monitoring of the cloud discontinuity to date to obtain a pioneering long-term characterisation of its main properties and to better constrain its recurrence and lifetime.
Methods. The dayside upper, middle, and nightside lower clouds were studied with images acquired by the Akatsuki Ultraviolet Imager (UVI), amateur observers, and SpeX at the NASA Infrared Telescope Facility (IRTF). Hundreds of images were inspected in search of the discontinuity events and to measure key properties such as its dimensions, orientation, and rotation period.
Results. We succeeded in tracking the discontinuity at the middle clouds during 109 days without interruption. The discontinuity exhibited properties nearly identical to measurements in 2016 and 2020, with an orientation of 91° ± 8°, length of 4100 ± 800 km, width of 500 ± 100 km, and a rotation period of 5.11 ± 0.09 days. Ultraviolet images during 13–14 June 2022 suggest that the discontinuity may have manifested at the top of the clouds during ~21 h as a result of an altitude change in the critical level for this wave, due to slower zonal winds.

Key words. waves – planets and satellites: atmospheres – planets and satellites: terrestrial planets – methods: data analysis

1. Introduction

From the surface up to ~90 km the general circulation of the atmosphere of Venus is dominated by a retrograde zonal superrotation whose speeds peak at the region of the clouds (45–70 km). Nevertheless, key aspects of its generation and maintenance are still poorly understood (Sánchez-Lavega et al. 2017), and present general circulation models (CGMs) still fail to accurately reproduce it (Lebonnois et al. 2013; Navarro et al. 2021). Recent works have provided new and solid evidence of the importance of planetary-scale waves at the upper clouds, such as the Y-feature (Boyer & Camichel 1961; Kouyama et al. 2012; Peralta et al. 2015) or the solar tides in maintaining the superrotation (Kouyama et al. 2015, 2019; Horinouchi et al. 2020; Fukuya et al. 2021). In addition, the waves excited below the clouds have been in the spotlight during the last years, thanks to recent reports of new waves discovered by the ongoing JAXA Akatsuki mission (Nakamura et al. 2016) and the earlier ESA Venus Express (Svedhem et al. 2007). Numerous stationary waves excited at the surface have been reported in images of the thermal emission of the upper clouds (Fukuhara et al. 2017; Peralta et al. 2017), 283 nm albedo at the cloud top (Kitahara et al. 2019), or in 2.02 μm dayside images (Sato et al. 2020).

Images of Venus that sense the middle and the lower clouds have revealed a disruption or discontinuity in their albedo–opacity (Peralta et al. 2020; Kardasis et al. 2022) linked to dramatic changes in the clouds' optical thickness and distribution of

aerosols (McGouldrick et al. 2021), and shown to be a recurrent atmospheric phenomenon missed for decades. Based on simulations with the Institut Pierre Simon Laplace (IPSL) Venus GCM (Scarica et al. 2019), it has been suggested that the discontinuity may be a new type of Kelvin wave feeding the superrotation with momentum from the deeper atmosphere, while its phase speeds along with its absence in observations of the upper clouds evidenced that this Kelvin wave might find its critical level below the top of the clouds (Peralta et al. 2020; Kardasis et al. 2022). Despite the potential relevance of this new wave, we have not been able to determine key aspects, such as its source of excitation, the excitation–dissipation heights, its long-term behaviour, and its recurrence in the Venus atmosphere.

Taking advantage of an excellent campaign of Venus observations undertaken during the year 2022 with a combined effort from the JAXA Akatsuki mission (Nakamura et al. 2007, 2016), NASA IRTF (Rayner et al. 2003), and amateur observers, we present the results of a long-term continuous monitoring of the cloud discontinuity and the first report of its propagation up to the top of the clouds. A description of the data sets and methods is introduced in Sect. 2, while the results and the discussion of the measured properties of the discontinuity and its manifestation at the top of the clouds can be consulted in Sect. 3. We finish with the main conclusions in Sect. 4.

2. Data sets and methods

As in previous works (Peralta et al. 2020; Kardasis et al. 2022), we searched for events of the discontinuity in images of Venus sensing the three main layers of the clouds (Titov et al. 2018): the dayside upper clouds (56.5–70 km above the surface), whose albedo at ~70 km can be observed with images taken at ultraviolet wavelengths (Ignatiev et al. 2009; Limaye et al. 2018); the dayside middle clouds (50.5–56.5 km), which can be observed at visible and near-infrared wavelengths (Hueso et al. 2015; Peralta et al. 2019a); and the nightside lower clouds (47.5–50.5 km), whose transparency–opacity to the deeper atmospheric thermal emission is observable in infrared atmospheric windows at 1.74, 2.26, and 2.32 μm (Satoh et al. 2017; Peralta et al. 2018).

2.1. Images obtained with IRTF/SpeX

The nightside lower clouds of Venus were explored using images of Venus taken from NASA's IRTF (Mauna Kea, Hawaii) with the guide camera of the instrument SpeX (Rayner et al. 2003) and contK (2.26 μm) and 1.74 μm filters. Our observations[1] covered the following dates: 2021 December 3–19 (12 nights), 2022 January 27–February 23 (23 nights), and 2022 March 5–12 (6 nights). During this period the phase angle of Venus varied within 140°–96° and the apparent size ranged 52–27 arcsec. Since the plate scale of SpeX is 0.116 arcsec per pixel, the spatial resolution of Venus in these images varied from 42 to 82 km per pixel. As in previous works (Peralta et al. 2019b, 2020), IRTF/SpeX images were corrected for the saturated dayside, stacked, navigated, and processed following the same procedure originally described in detail in Peralta et al. (2018). Unfortunately, an accurate radiometric calibration was not possible due to a persistent problem of light contamination from the saturated dayside of the planet similar to that affecting images by Akatsuki/IR2 (Satoh et al. 2022).

[1] Data available upon reasonable request.

Table 1. Discontinuity events observed during February–July 2022.

Date/time (UT)	Clouds [(a)]	Wavelength [(b)]	Observer
2022-02-04 16:55	Lower	2.26 μm	IRTF/SpeX
2022-05-05 04:36	Middle	>742 nm	C. Foster
06:13	Middle	820–920 nm	A. Cidadão
2022-05-15 04:29	Middle	>742 nm	C. Foster
08:16	Middle	820–920 nm	A. Cidadão
2022-05-25 04:41	Middle	>742 nm	C. Foster
07:58	Middle	820–920 nm	A. Cidadão
2022-05-30 05:14	Middle	>742 nm	C. Foster
09:06	Middle	>685 nm	L. S. Viola
2022-06-04 05:09	Middle	820–920 nm	L. Morrone
09:52	Middle	820–920 nm	A. Cidadão
2022-06-13 14:05	Upper	345–380 nm	VCO [(c)]/UVI
2022-06-14 23:05			
2022-06-14 05:16	Middle	820–920 nm	L. Morrone
2022-06-19 05:52	Middle	820–920 nm	L. Morrone
06:48	Middle	820–920 nm	A. Cidadão
2022-06-24 05:46	Middle	820–920 nm	L. Morrone
07:36	Middle	820–920 nm	A. Cidadão
2022-07-09 06:33	Middle	820–920 nm	A. Cidadão
2022-07-13 10:33	Middle	820–920 nm	A. Cidadão
2022-07-18 11:57	Middle	820–920 nm	A. Cidadão
2022-07-23 06:27	Middle	820–920 nm	L. Morrone
07:54	Middle	820–920 nm	A. Cidadão
2022-07-28 09:21	Middle	820–920 nm	A. Cidadão

Notes. [(a)]Approximate level sensed: dayside upper clouds (56.5–70 km above the surface), dayside middle clouds (50.5–56.5 km), and nightside lower clouds (47.5–50.5 km). [(b)]Filters used: contK (2.22–2.32 μm), Astronomik ProPlanet 742 IR-pass filter (>742 nm), Baader SLOAN/SDSS $z' - s'$ (820–920 nm), Baader IR-Pass Filter (>685 nm), and VCO/UVI 365 nm (345–380 nm). [(c)]Venus Climate Orbiter: Previous name of Akatsuki (Nakamura et al. 2007).

2.2. Images obtained by amateur observers

To study the presence of the discontinuity on the dayside middle clouds, we used images of Venus acquired by amateur observers located in Italy, Portugal, South Africa, Australia, Estonia, and Taiwan. We obtained the images directly from some of the observers or through the Venus section of ALPO-Japan[2] (Sato 2018). These consist of stacks of thousands of images acquired during time intervals rarely longer than 5 min (see lucky imaging procedure in Kardasis et al. 2022), and they were captured using small telescopes with diameters typically in the range 203–355 mm, observing at wavelengths >685 nm in all the cases by means of high-pass and band-pass filters (the most-used filters are detailed in Table 1 of Kardasis et al. 2022). After a careful selection, we inspected a total of 319 images covering nearly every day from 2022 March 13 until July 31. During this period the phase angle of Venus varied within 95°–32° and the apparent size ranged 27–11 arcsec. For wavelengths of ~700 nm and telescope of 355 mm diameter we would expect a nominal resolution of ~0.5 arcsec for each individual image, and 350–860 km per pixel along the mentioned observing period. Since the lucky imaging has demonstrated superresolution capabilities and improves the resolution up to a factor of four in poor seeing conditions (Farsiu et al. 2004; Law et al. 2006; Sánchez-Lavega et al. 2016; Peralta et al. 2017), we can assume a conservative improvement of a factor of two for the

[2] http://alpo-j.sakura.ne.jp/Latest/Venus.htm

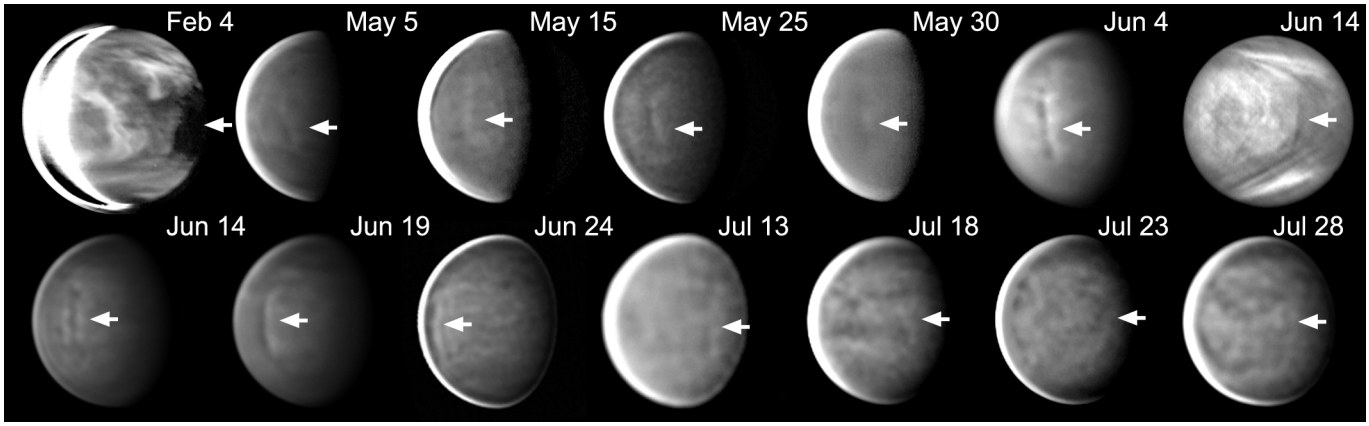

Fig. 1. Examples of discontinuity events during 2022. The discontinuity was apparent on the nightside lower clouds with 2.26 μm images from IRTF/SpeX taken on February 4, and at the dayside middle clouds as observed in images by amateur observers taken with filters covering wavelengths 700–900 nm from May to July 2022. During June 14, Akatsuki/UVI images at 365 nm suggest that the discontinuity was propagating simultaneously at the upper and middle clouds (last image in upper row). All the images were high-pass filtered to enhance cloud details.

stacked images, implying spatial resolutions within 175–430 km per pixel.

2.3. Images obtained with Akatsuki/UVI and LIR

The level of the upper clouds was studied with images taken by two instruments on board the Akatsuki orbiter: 365 and 283 nm images by the Ultraviolet Imager (UVI) (Yamazaki et al. 2018) were used to explore the cloud patterns and zonal winds at the top of the dayside upper clouds (~70 km) while 10 μm images by the Longwave Infrared camera (LIR) can sense thermal contrasts within a wider altitude range of 60–75 km (Taguchi et al. 2007) which vary with observed emission angle (Kouyama et al. 2017; Akiba et al. 2021). UVI and LIR data consisted of L2b and L3bx products (Ogohara et al. 2017; Murakami et al. 2019) from the mission internal release[3] v20220901, and the images matched the same observing period as for the middle clouds with amateur observations. The imagery data set finally selected covered from 2022 April 15 until July 30 (Akatsuki orbits 212–221), with the spatial resolution at lower latitudes of Venus varying 75–10 km per pixel in UVI images and 320–40 km per pixel in LIR images. We explored a total of 928 UVI images at 365 nm (similar number of 283 nm images) and 623 LIR images, although in the latter case we only examined LIR images acquired during confirmed events of the discontinuity (see Sect. 3.1).

2.4. Measurement of speeds

Prior to measurements, all the images were geometrically projected onto an equirectangular (cylindrical) geometry with an angular resolution equivalent to the best resolution in the original images. To measure winds and the phase speed of the discontinuity, we applied the manual method by Sánchez-Lavega et al. (2016) and another technique consisting of a manual search of cloud tracers followed by a fine adjustment using automatic template matching based on phase correlation, which is visually accepted or rejected by a human operator (Peralta et al. 2018, Sect. 2.3).

To achieve a more accurate characterisation of the difference between the discontinuity phase speed and zonal winds (Peralta et al. 2020; Kardasis et al. 2022), the phase speed of the discontinuity was measured by comparing its position after one or two full revolutions around the planet Venus, allowing us to achieve an accuracy of 0.2–2.7 m s^{-1}. Concerning the measurement of wind speeds at the nightside lower clouds, we combined pairs of stacked images from SpeX typically separated by 90–155 min, which enabled us to infer winds with errors within 3–8 m s^{-1}. In the case of the UVI 365 nm images, we obtained wind speeds with errors ranging 2–11 m s^{-1} by considering pairs of images acquired when Akatsuki approached or receded from its orbital pericentre or when cloud tracers could be tracked during 3–5 hours. We excluded our wind measurements for dayside middle clouds since the worse spatial resolution of amateur images generally precluded speeds with errors below 40 m s^{-1}. The speeds in Sect. 3 were calculated as the mean and standard deviation for speeds of individual tracers between 30°N and 30°S.

3. Results

3.1. Properties of the discontinuity

We observed the nightside lower clouds of Venus between 2021 December 3 and 2022 March 12, while the dayside clouds were studied between 2022 March 13 and July 31. Table 1 describes the discontinuity events identified during these campaigns, while Figs. 1 and A.1 exhibit images of these events. Despite the number of observations with IRTF/SpeX between December 2021 and March 2022, only one positive event was confirmed with the cloud discontinuity with a length of 2900 ± 700 km, width of 400 ± 40 km, orientation of 91° ± 8°, and propagating at a phase speed of −79 ± 6 m s^{-1} (10 ± 8 m s^{-1} faster than winds), and faster than the speed −68 ± 9 m s^{-1} reported in 2016–2018 (Peralta et al. 2020). An abrupt change in the clouds' opacity was also observed in February 15 and 20 (see Fig. B.1), suggesting the reappearance of the first discontinuity after several full revolutions. Nevertheless, their zonal speeds matched those of the background winds within the error bars, and we decided to discard them from the analysis. The fast increase in zonal wind speeds after February 4 (see Fig. 2a) suggests a probable dissipation of the wave leaving a persistent reminiscence of its effect on the clouds' opacity.

A total of 13 events were confirmed in the set of amateur images sensing the dayside middle clouds of Venus between

[3] Available via Data ARchives and Transmission System (DARTS) by ISAS/JAXA Center for Science-satellite Operation and Data Archive (C-SODA), and NASA PDS Atmospheres Node.

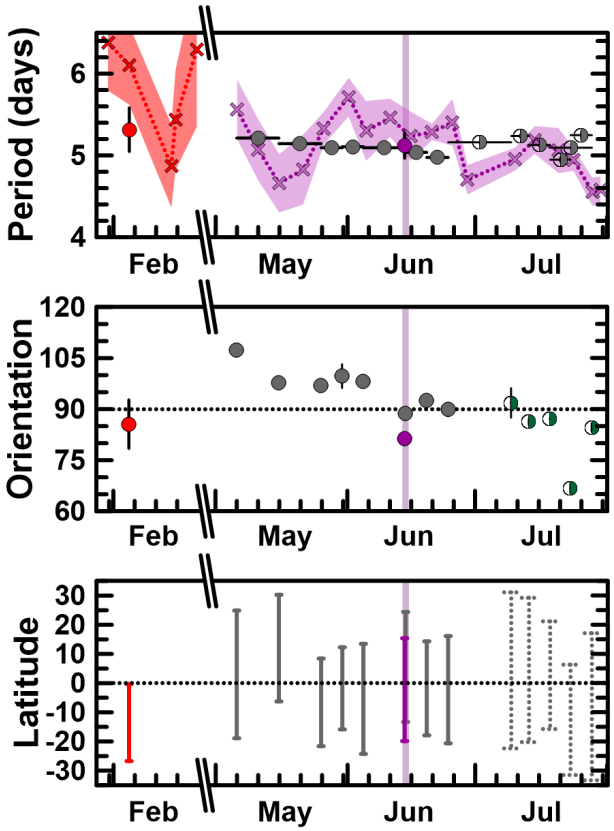

Fig. 2. Properties of the discontinuity during 2022. Panel (a) exhibits the rotation period (as terrestrial days) for the discontinuity zonal phase speed (circles) and zonal winds (crosses) along with their errors (bars for phase speeds, shadowed areas for winds). Red represents winds and discontinuity events at the nightside lower clouds; grey and purple correspond to dayside middle and upper clouds, respectively. Panel (b) displays the orientation of the discontinuity (circles) as degrees relative to the equator and/or parallels. Panel (c) shows the meridional coverage of the discontinuity (vertical bars). Since the discontinuity seemed to weaken during July 2022, data is displayed as half-filled circles (period and orientation) and dotted bars (meridional coverage). The time frame in light violet corresponds to the event when the discontinuity simultaneously manifested at the upper and middle clouds.

April and July 2022 (see Table 1 and Fig. 1). On average, the discontinuity at the middle clouds exhibited a mean length of 4100 ± 800 km, width of 500 ± 100 km, average phase speed of $c = -84 \pm 2\,\mathrm{m\,s^{-1}}$ and rotation period of 5.11 ± 0.09 terrestrial days. These values match the results from the Akatsuki/IR1 images during 2016 ($-74 \pm 9\,\mathrm{m\,s^{-1}}$ and 4.7 ± 0.4 days; see Peralta et al. 2020) and amateur images during March–April 2020 ($-84.9 \pm 0.4\,\mathrm{m\,s^{-1}}$ and 5.08 ± 0.03 days; see Kardasis et al. 2022).

The time evolution of the discontinuity zonal phase speed, orientation relative to the equator, and meridional coverage is displayed in Fig. 2. Regarding the night lower clouds, the low number of discontinuity events observed during February 2022 might be related to a potential dissipation of the wave, due to the fast increase in the zonal winds after February 4, perhaps caused by an equatorial jet (Horinouchi et al. 2017). For the events at the dayside middle clouds, two periods can be distinguished. From May to June 2022 the discontinuity exhibits its strongest perturbation over the clouds' albedo, especially between May 30 and June 24 (see Fig. 1) when its characteristic dark-to-bright streak pattern is clearly visible (Kardasis et al. 2022). During this period we also observe that the discontinuity seems to rotate faster as it becomes more perpendicular to the equator (see Figs. 2a–b). During July 2022, the rotation period and the orientation exhibit a higher variability, accompanied by a less pronounced alteration in the cloud albedo (see Fig. 1). Although this might be interpreted as an episode of gradual weakening of the discontinuity, we cannot rule out an observational bias since during July 2022 the spatial resolution becomes comparable to the discontinuity width (500 ± 100 km).

3.2. Possible discontinuity at the top of the clouds

Given that it could not be identified in the images of the upper clouds taken by Akatsuki during 2016, the discontinuity was interpreted as a Kelvin-type wave that propagates at the deeper clouds and probably dissipates before arriving at the upper clouds (Peralta et al. 2020), which is supported by zonal phase speeds faster than winds at the deeper clouds and slower than winds at the top of the clouds (Kardasis et al. 2022). During June 13–14 (see Table 1 and Fig. 1) and probably also on May 30 (see Fig. C.1), a discontinuity-like pattern propagating $10 \pm 8\,\mathrm{m\,s^{-1}}$ faster than the background winds was observed in UVI images at 365 and 283 nm (Fig. 1), but not in 10 μm thermal images from LIR (presumably due to their worse spatial resolution during these dates). This pattern became apparent at the top of the clouds on June 13 at about 20:00 UT near the border of the Y-feature (which was also present), gradually intensifying and then vanishing on June 14 17:00 UT (see animated Fig. 3).

Although the ultraviolet albedo sometimes exhibits sharp patterns, the event on June 13–14 shares with the discontinuity at the middle clouds location, rotation period, orientation and latitudinal coverage, while the zonal winds at the top of the clouds are slow enough to change the altitude of the critical level and facilitate the vertical propagation of the Kelvin wave (see Fig. 2). Using the amateur image acquired in 2022 June 14 05:15:50 UT and the UVI image at 06:04:44 UT (see Fig. C.1), we derived the position of the discontinuity at the middle clouds when the UVI image was taken, considering that $c - 84 \pm 2\,\mathrm{m\,s^{-1}}$. As a result, we inferred a phase difference $\Delta\varphi = 7 \pm 2°$ (i.e., ~700 ± 200 km) for the discontinuity at both levels. Assuming that the top of the clouds and the middle clouds are located at 74 ± 1 km (Ignatiev et al. 2009) and 63 ± 5 km (Khatuntsev et al. 2017), respectively, the altitude difference is $\Delta h = 11 \pm 6$ km and the angle between the wave vector and the horizontal plane ($\tan\phi = \frac{\Delta\varphi}{\Delta h}$) will be $\phi = 89 \pm 1°$. In addition, given that $\tan\phi = \frac{\lambda_x}{\lambda_z}$ (Gubenko et al. 2011) and considering that the width of the discontinuity is representative of the zonal wavelength ($\lambda_x = 500 \pm 100$ km), the vertical wavelength will be $\lambda_z = 9 \pm 2$ km.

4. Conclusions

Thanks to the coordinated observations by the JAXA Akatsuki mission and to ground-based professional and amateur observers during the first half of 2022, we have presented the longest uninterrupted study of the cloud discontinuity of Venus to date, extending 109 days from 2022 March 13 to July 31 and covering several cloud layers of the atmosphere.

The nightside lower clouds were explored by means of 2.26 μm images taken by IRTF/SpeX over 41 days from December 2021 to March 2022. Nevertheless, the discontinuity seems to manifest only once prior to an intensification of the zonal winds at lower latitudes. The middle and upper clouds were studied in 2022 March–July with amateur and Akatsuki/UVI

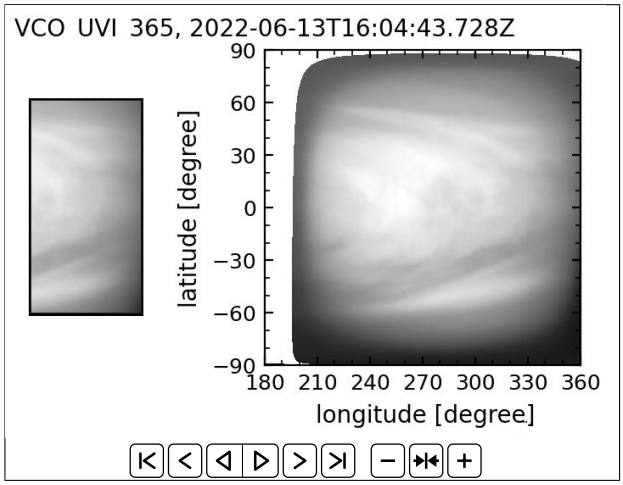

Fig. 3. Evolution of the discontinuity-like pattern observed at the top of the clouds with Akatsuki/UVI images. This interactive animation exhibits the morphological evolution (left panel) and propagation (right panel) of the discontinuity during the event of its apparent manifestation at the upper and lower clouds (see Table 1 and Fig. 1). The animation was built with geometrical projections (Ogohara et al. 2017, see level 3 data) of Akatsuki/UVI images taken at 365 nm every ∼2 hours from 2022 June 13 at 16:05 UT until June 14 at 23:05 UT. These equirectangular projections consist of longitude-latitude maps with a fixed resolution of 0.125° (2880 × 1440 grids for 360° longitude and 180° latitude). The propagation of the discontinuity (right panel) is shown for maps covering latitudes 90°N–90°S and longitudes 180°–360°. For its morphological evolution (left panel) we used 60°N–60°S projections shifted to show the discontinuity at rest. The moving white spot corresponds to dead pixels. No photometric correction was applied.

observations, respectively. As many as 13 discontinuity events were identified at the middle clouds, exhibiting an average length of 4100 ± 800 km, width of 500 ± 100 km, and a mean rotation period of 5.11 ± 0.09 terrestrial days, a period identical to estimates from 2016 (Peralta et al. 2020) and 2020 (Kardasis et al. 2022). For the first time we have reported the possible manifestation of the discontinuity at the top of the clouds during ∼21 h, suggesting that the critical level for this Kelvin wave ascended due to the slower winds at the top of the clouds. Nonetheless, further research into the atmospheric conditions is required to explain why the discontinuity seemed absent at the cloud tops on other dates with slower winds.

Even though the discontinuity was not identified in Akatsuki/LIR images, future Akatsuki observations might accomplish new positive identifications if discontinuity events occur during pericentric observations (when Akatsuki images have better spatial resolution). In addition, a revisit of Venus ultraviolet images during past episodes of slower winds may reveal new discontinuity events with Akatsuki (Horinouchi et al. 2018) and previous space missions, such as the NASA Pioneer Venus or the ESA Venus Express (Rossow et al. 1990; Hueso et al. 2015; Khatuntsev et al. 2013), allowing us to characterise its recurrence with better accuracy.

Acknowledgements. J.P. thanks EMERGIA funding from Junta de Andalucía in Spain (code: EMERGIA20_00414). I.G.-L. and A.S.-L. were supported by Grant PID2019-109467GB-I00 funded by MCIN/AEI/10.13039/501100011033/ and by Grupos 1128 Gobierno Vasco IT1742-22. We thank the members of JAXA's Akatsuki mission and Visiting Astronomers at the Infrared Telescope Facility operated by the University of Hawaii under contract 80HQTR19D0030 with NASA. This research would have been impossible without the many amateur observers who observed Venus intensively during the investigated period and shared their images, although we would like to highlight contributions from M. A. Bianchi, G. Calapai, D. Kananovich, N. MacNeill, V. Mirabella, W. M. Lonsdale, R. Sedrani, L. S. Viola and G. Z. Wang. Finally, We thank the two anonymous reviewers whose comments and suggestions helped improve and clarify this manuscript.

References

Akiba, M., Taguchi, M., Fukuhara, T., et al. 2021, J. Geophys. Res. (Planets), 126
Boyer, C., & Camichel, H. 1961, Ann. d'Astrophys., 24, 531
Farsiu, S., Robinson, M. D., Elad, M., & Milanfar, P. 2004, IEEE Trans. on Image Proces., 13, 1327
Fukuhara, T., Futaguchi, M., Hashimoto, G. L., et al. 2017, Nat. Geosci., 10, 85
Fukuya, K., Imamura, T., Taguchi, M., et al. 2021, Nature, 595, 511
Gubenko, V. N., Pavelyev, A. G., Salimzyanov, R. R., & Pavelyev, A. A. 2011, Atmos. Measure. Tech., 4, 2153
Horinouchi, T., Murakami, S., Satoh, T., et al. 2017, Nat. Geosci., 10, 646
Horinouchi, T., Kouyama, T., Lee, Y. J., et al. 2018, Earth Planets Space, 70, 10
Horinouchi, T., Hayashi, Y.-Y., Watanabe, S., et al. 2020, Science, 368, 405
Hueso, R., Peralta, J., Garate-Lopez, I., Bandos, T. V., & Sánchez-Lavega, A. 2015, Planet. Space Sci., 113, 78
Ignatiev, N. I., Titov, D. V., Piccioni, G., et al. 2009, J. Geophys. Res. (Planets), 114, E00B43
Kardasis, E. M., Peralta, J., Maravelias, G., et al. 2022, Atmosphere, 13, 348
Khatuntsev, I. V., Patsaeva, M. V., Titov, D. V., et al. 2013, Icarus, 226, 140
Khatuntsev, I. V., Patsaeva, M. V., Titov, D. V., et al. 2017, J. Geophys. Res. (Planets), 122, 2312
Kitahara, T., Imamura, T., Sato, T. M., et al. 2019, J. Geophys. Res. (Planets), 124, 1266
Kouyama, T., Imamura, T., Nakamura, M., Satoh, T., & Futaana, Y. 2012, Planet. Space Sci., 60, 207
Kouyama, T., Imamura, T., Nakamura, M., Satoh, T., & Futaana, Y. 2015, Icarus, 248, 560
Kouyama, T., Imamura, T., Taguchi, M., et al. 2017, Geophys. Res. Lett., 44, 12
Kouyama, T., Taguchi, M., Fukuhara, T., et al. 2019, Geophys. Res. Lett., 46, 9457
Law, N. M., Mackay, C. D., & Baldwin, J. E. 2006, A&A, 446, 739
Lebonnois, S., Lee, C., Yamamoto, M., et al. 2013, eds. L. Bengtsson, R. M. Bonnet, D. Grinspoon, et al. Models of Venus Atmosphere (, 129
Limaye, S. S., Watanabe, S., Yamazaki, A., et al. 2018, Earth Planets Space, 70, 38
McGouldrick, K., Peralta, J., Barstow, J. K., & Tsang, C. C. C. 2021, Planet. Sci. J., 2, 153
Murakami, S., Yamamoto, Y., McGouldrick, K., et al. 2019, in JAXA Data Archives and Transmission System (Japan Aerospace Exploration Agency: Institute of Space and Astronautical Science)
Nakamura, M., Imamura, T., Ueno, M., et al. 2007, Planet. Space Sci., 55, 1831
Nakamura, M., Imamura, T., Ishii, N., et al. 2016, Earth Planets Space, 68, 1
Navarro, T., Gilli, G., Schubert, G., et al. 2021, Icarus, 366
Ogohara, K., Takagi, M., Murakami, S.-Y., et al. 2017, Earth Planets Space, 69, 167
Peralta, J., Sánchez-Lavega, A., López-Valverde, M. A., Luz, D., & Machado, P. 2015, Geophys. Res. Lett., 42, 705
Peralta, J., Hueso, R., Sánchez-Lavega, A., et al. 2017, Nat. Astron., 1, 0187
Peralta, J., Muto, K., Hueso, R., et al. 2018, ApJS, 239, 17
Peralta, J., Iwagami, N., Sánchez-Lavega, A., et al. 2019a, Geophys. Res. Lett., 46, 2399
Peralta, J., Sánchez-Lavega, A., Horinouchi, T., et al. 2019b, Icarus, 333, 177
Peralta, J., Navarro, T., Vun, C. W., et al. 2020, Geophys. Res. Lett., 47
Rayner, J. T., Toomey, D. W., Onaka, P. M., et al. 2003, PASP, 115, 362
Rossow, W. B., del Genio, A. D., & Eichler, T. 1990, J. Atmos. Sci., 47, 2053
Sánchez-Lavega, A., Peralta, J., Gomez-Forrellad, J. M., et al. 2016, ApJ, 833, L7
Sánchez-Lavega, A., Lebonnois, S., Imamura, T., Read, P., & Luz, D. 2017, Space Sci. Rev., 212, 1541
Sato, T. 2018, J. Assoc. Lunar Planet. Obs. Stroll. Astron., 60, 20
Sato, T. M., Satoh, T., Sagawa, H., et al. 2020, Icarus, 345
Satoh, T., Sato, T. M., Nakamura, M., et al. 2017, Earth Planets Space, 69, 154
Satoh, T., Uemizu, K., Ueno, M., Kimata, M., & Sato, T. M. 2022, in SPIE Conf. Ser., eds. S. R. Babu, A. Hélière, & T. Kimura, 12264, 122640H.
Scarica, P., Garate-Lopez, I., Lebonnois, S., et al. 2019, Atmosphere, 10, 584
Svedhem, H., Titov, D. V., McCoy, D., et al. 2007, Planet. Space Sci., 55, 1636
Taguchi, M., Fukuhara, T., Imamura, T., et al. 2007, AdSpR, 40, 861
Titov, D. V., Ignatiev, N. I., McGouldrick, K., Wilquet, V., & Wilson, C. F. 2018, Space Sci. Rev., 214, 126
Yamazaki, A., Yamada, M., Lee, Y. J., et al. 2018, Earth Planets Space, 70, 23

Appendix A: Discontinuity events projected

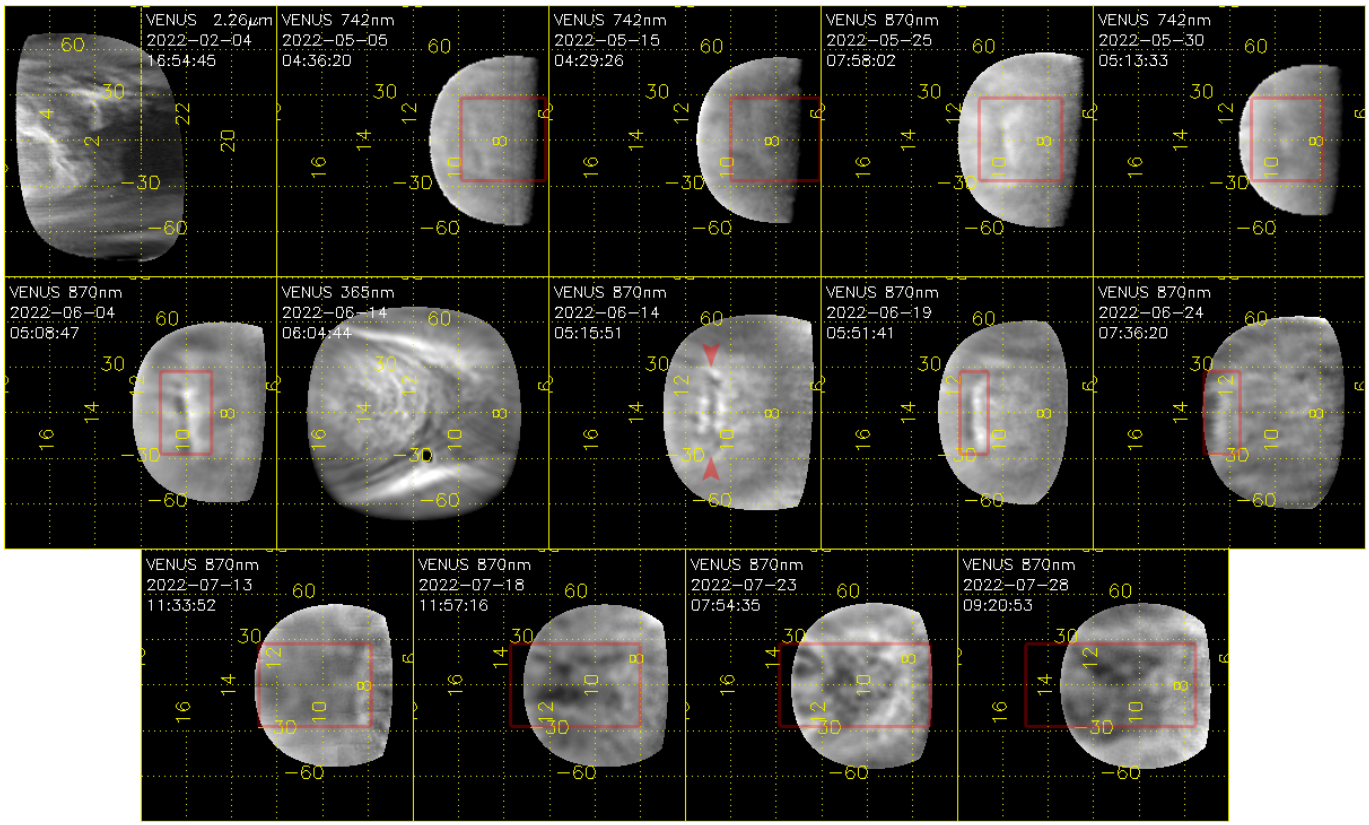

Fig. A.1. Geometrical projections of discontinuity events during 2022. This supporting figure displays the same examples of discontinuity as in Figure 1, but as equirectanguar (cylindrical) projections with an angular resolution of 0.75° per pixel. The images are projected for latitudes 90°N–90°S (vertical axis) and local hour coordinates (horizontal axis). The discontinuity was apparent on the nightside lower clouds with 2.26 μm images from IRTF/SpeX taken on February 4, and on the dayside middle clouds as observed with images by amateur observers taken with filters covering wavelengths 700–900 nm during May 5, 15, 25, 30; June 14, 19, 24; and July 13, 18, 23, 28. Exceptionally, the discontinuity seemed to manifest at the top of the dayside clouds with Akatsuki/UVI images at 365 nm during June 14. The red rectangles represent the areas where we expect to find the discontinuity when considering June 14 as the reference position and mean rotation period of 5.11 ± 0.09 terrestrial days.

Appendix B: The discontinuity at the lower clouds

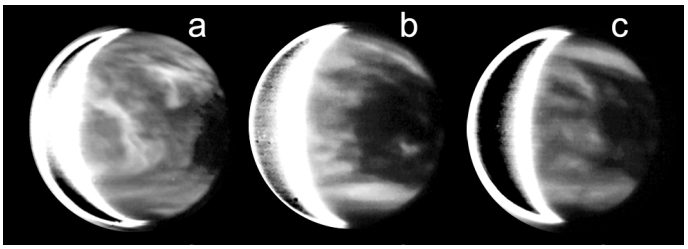

Fig. B.1. Evolution of the cloud discontinuity at the nightside lower clouds. These 2.26μm images from IRTF/SpeX display the manifestation of the discontinuity at the nightside lower clouds on 2022 February 4 (a). Even though the abrupt change in the clouds' opacity on February 15 (b) and 20 (c) suggest the reappearance of the first discontinuity after several full revolutions, their zonal speeds match those of the background wind within the error bars. The fast increase in zonal wind speeds after February 4 (see Fig. 2a) suggests a probable dissipation of the wave, while leaving a persistent artefact of its effect on the opacity of the nightside lower clouds.

Appendix C: The discontinuity at two cloud layers

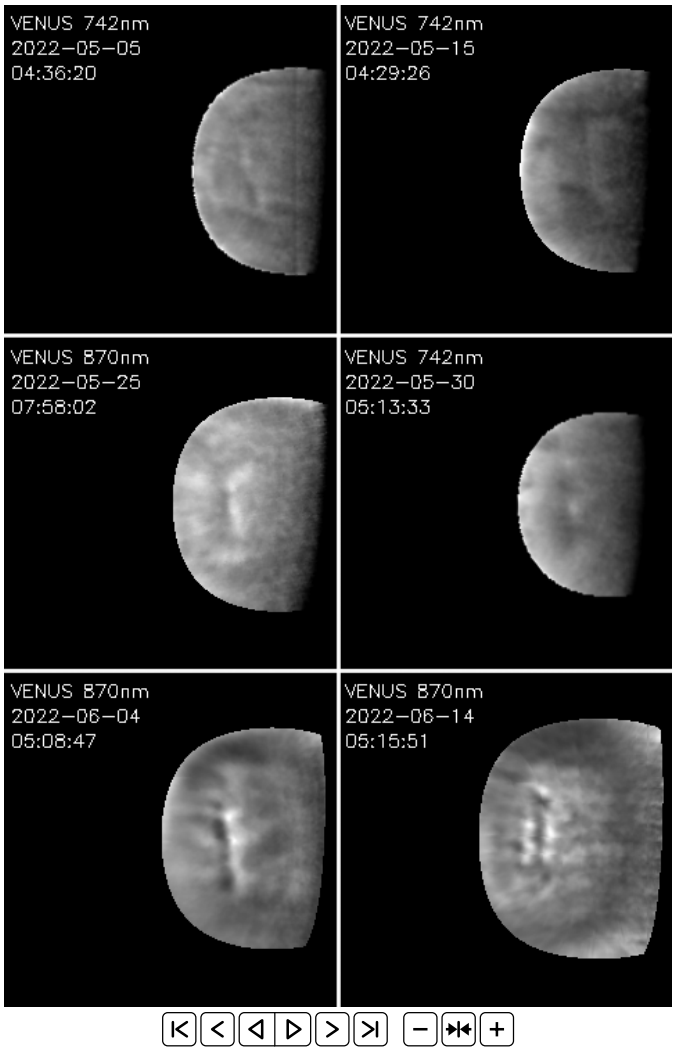

Fig. C.1. Cloud layers during six discontinuity events in 2022. By means of images acquired within less than 1 hour of difference, this interactive animation allows a comparison of the patterns at the *top of the clouds* (Akatsuki/UVI 365 nm images) when the discontinuity was apparent in the images of the *middle clouds*. As in Fig. A.1, 90°N–90°S projections in local hour coordinates and resolution of 0.75° per pixel are shown. Coordinate grid suppressed for a better visualisation.